

*Combustion synthesis and characterization of Fe₂O₃-ZrO₂
nanocomposite oxides*

*A Dissertation
Submitted in partial fulfillment*

**FOR THE DEGREE OF
Master of Science in Chemistry**

Under Academic Autonomy

NATIONAL INSTITUTE OF TECHNOLOGY, ROURKELA

Submitted by

SUJAN DUTTA
ROLL.NO: 408CY105

Under the Guidance of

Dr. B. G. Mishra



**DEPARTMENT OF CHEMISTRY
NATIONAL INSTITUTE OF TECHNOLOGY
ROURKELA, ORISSA 769 008**

CERTIFICATE

Dr. Braja Gopal Mishra
Associate Professor
Dept. of Chemistry



This is to certify that the dissertation entitled “*Combustion synthesis and characterization of $Fe_2O_3-ZrO_2$ nanocomposite oxides*” being submitted by **Sujan Dutta** to the Department of Chemistry, National Institute of Technology, Rourkela, Orissa, for the award of the degree of Master of Science is a record of bonafide research work carried out by him under my supervision and guidance. I am satisfied that the dissertation report has reached the standard fulfilling the requirements of the regulations relating to the nature of the degree.

N.I.T. Rourkela.

Date:

Dr. Braja Gopal Mishra
Supervisor

Acknowledgements

I take this opportunity to express my deep appreciations and indebtedness to Dr. Braja Gopal Mishra, Department of Chemistry, National Institute of Technology, Rourkela, Orissa, for all of his invaluable guidance, continuous encouragement and sharing of frustrations as well as enjoyment throughout this course of research work. Indeed, the experience of working under him is one of that I will cherish forever.

It is my great pleasure to acknowledge to Prof. R.K. Patel, Head of the Chemistry Department, National Institute Of Technology, Rourkela for providing me the necessary facilities for this research work.

I am indebted to all faculty and staff members of Department of Chemistry, N.I.T, Rourkela, for their help.

I extend my thanks to my laboratory colleague Mr. Satish Samantaray and my classmate Mr.Sudhir Kr Sahoo who were working with me with every difficulty, which I have faced and their constant efforts and encouragement was the tremendous sources of inspiration for me.

Finally, I wish to thank all of my friends for making my stay in this institute a memorable experience.

Sujan Dutta

CHAPTER 1

INTRODUCTION

1.1 General Introduction

Metals and their oxides act as a heterogeneous catalysis in many industrial chemical processes. Since the reaction rate on a catalyst surface depends upon the total surface area and the number of active sites present, a good catalyst is required to possess smaller particles and high surface area. For example, in the Haber process finely divided iron serves as a catalyst for the synthesis of ammonia from nitrogen and hydrogen. Precious metals including Pt, Pd, Rh, Ru and Ni are employed in various catalytic processes such as naphtha reforming, abatement of automobile emissions, hydrogenation of CO and fats [1]. Another most important class of materials which have been used as heterogeneous catalyst is the metal oxides. Metal oxides generally exhibit both electron and proton transfer abilities and can be used as catalysts in redox as well as acid-base reactions. The redox properties of oxides are exploited in catalytic purification systems for complete oxidation of toxic materials [2,3]. The oxide systems with inherent redox properties have also been used for selective oxidation of organic compounds and to synthesize important fine chemicals such as aldehyde, acids and nitriles [2, 3]. The surface acid-base properties of oxides have been taken advantage in carrying out selective organic transformations. The physicochemical characteristics and the catalytic activity of a metal oxide depend upon several intrinsic and extrinsic factors. Among the extrinsic factors, the most important is the method of preparation of the oxide. Many methods have been reported in the literature for the preparation of the metal oxides with desired properties. However, most of the methods used for preparation of oxides such as precipitation, malaxing, thermal treatment of precursors, high energy ball milling are multistep processes involving a lot of parameters. For example for preparation of oxides by coprecipitation method, the rate of hydrolysis, the rate of addition of the precipitating agent, the pH of the solution, the stirring rate, the drying temperature and calcination temperature and environment are important factors which can influence the final property of the oxide. In order to reproduce the exact nature of the oxide, these factors have to be precisely controlled. However, precision of all these factors and parameters is a remote possibility which consequently affects the

reproducibility of the synthesis. The following figure 1.1 shows schematically the different steps involved in some of the commonly employed synthetic methods for oxides.

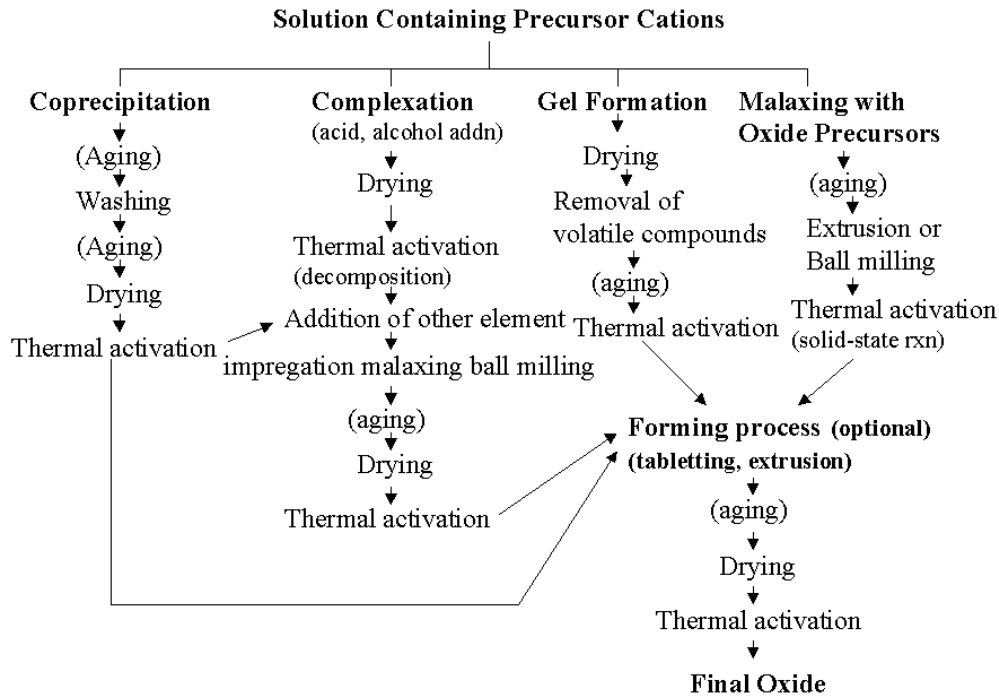


Figure 1.1. different steps involved in some of the commonly employed synthetic methods for oxides

In recent years, there are efforts to synthesize oxides with reproducible properties by employing novel methods which involve fewer processing steps. The most prominent among them is combustion synthesis which is a single step process.

1.2 Combustion Synthesis Method

Combustion synthesis (CS) or self-propagating high-temperature synthesis (SHS) is an effective, low-cost method for production of various industrially useful materials [4,5]. This field is important for development of new catalysts and nanocarriers with properties better than those for similar traditional materials. This method is described as a quick, straightforward preparation process to produce homogeneous, well crystalline and unagglomerated multicomponent oxide ceramic powders, without the intermediate decomposition and/or calcination step [4, 5]. Solution combustion synthesis (SCS) a modified form of combustion synthesis is a versatile, simple and rapid process, which allows effective synthesis of a variety of nanosize materials [4]. This

process involves a self-sustained reaction in homogeneous solution of different oxidizers (e.g., metal nitrates) and fuels (e.g., urea, glycine, hydrazides). Depending on the type of the precursors, as well as on conditions used, the SCS may occur as either volume or layer-by-layer propagating combustion modes. This process not only yields nanosize oxide materials but also allows uniform (homogeneous) doping of trace amounts impurity ions in a single step. The combustion reaction is usually initiated in a muffle furnace or on a hot plate at low temperature of about 773 K or less; much lower than the phase transition of the target material. In a typical reaction, a homogeneous mixture of water, metal nitrate precursors and fuel are allowed to dehydrate leading to the exothermic decomposition of the fuel. The chemical energy released from the exothermic reaction between the metal nitrate and fuel appears as large amount of heat which is sufficient enough to raise the temperature of the system to higher value (>1600 K) for a short duration of time. As a result of decomposition of the fuel and the nitrate a sudden evolution of large volume of gas occurs. This makes large particles or agglomerates get disintegrated leading to the formation of materials, which can be easily crushed to obtain fine particles.

1.3 Zirconia as support and catalyst-an introduction

Among the metal oxides which are widely employed as catalysts and support, the most prominent are silica, alumina and zirconium dioxide. Zirconium dioxide is an important oxide which has been used extensively for heterogeneous catalytic reactions. Application of zirconium dioxide has been quite promising in catalysis and many other areas due to its versatile structural and surface chemical properties as well as good thermal stability [6, 7]. It has been reported as a better catalyst and catalyst support compared to classical materials such as Al_2O_3 , SiO_2 and TiO_2 [8]. The modified versions of zirconium dioxide, viz. the sulfated ZrO_2 , zirconia substituted mixed oxides such as $\text{Ce}_x\text{Zr}_{1-x}\text{O}_2$ solid solutions ($0 \leq x \leq 1$), various transition metal stabilized zirconia and hydrous zirconium oxide have been reported to be effective for several organic reactions, combustion and gas phase reactions [8,9]. The partial substitution of ZrO_2 into CeO_2 improves the thermal stability, oxygen storage capacity and redox properties of ceria considerably. This is considered as a significant contribution to three-way catalyst (TWC) technology [9]

1.4 Structure properties and phase transformation of ZrO_2

ZrO₂ is a high temperature ceramic oxide. Its physical properties include high melting point (2710oC) and is resistant to chemical attack by strong acids. Zirconia is also stable in oxidizing environments, allows oxygen diffusion through its bulk, exhibits good thermal conductivity, and is electrically insulating. These properties enable Zirconia to be used as an abrasive, as a hard resistant coating for cutting tools, in oxygen electrodes and sensors, and in high temperature engine components. Structurally, Zirconia exists in three polymorphic forms [10, 11]. The high temperature stable form is cubic and possesses a fluorite structure. The Fluorite structure of Zirconia is shown in Figure 1.2.

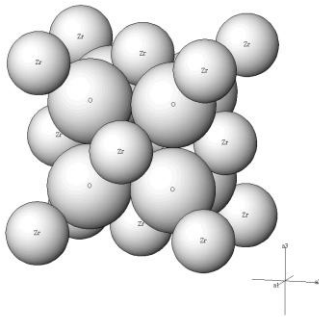
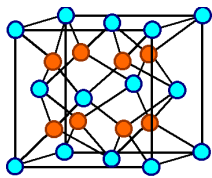
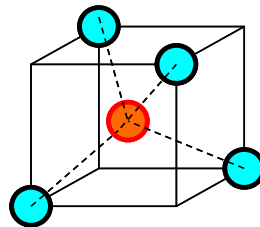


Figure 1.2. The hard sphere model for the fluorite structure of ZrO₂.

The structure of ZrO₂ can be described as the Zr⁴⁺ ions forming a cubic close pack structure (FCC lattice) with the O²⁻ ions occupying all the tetrahedral holes. In the FCC structure, the Zr⁴⁺ ions occupy all the corners and the face center position of the cube. If the cube is divided into eight symmetric smaller cubes through its centre, then the oxygen ions occupy the centers of all the smaller cubes (figure 1.3).



(a)



(b)

Figure1. 3. (a) The fluorite structure of ZrO₂ and (b) The tetrahedral sites (Red Dot: O²⁻ and cyan dot: Zr⁴⁺)

With decreasing temperature, ZrO_2 undergoes a cubic to tetragonal (c \rightarrow t) phase transition at around 2380°C and a tetragonal to monoclinic (t \rightarrow m) phase transition at around 1205°C [10, 11]. At the cubic to tetragonal phase transition, the fluorite cubic structure distorts to the tetragonal structure with the tetragonal c-axis parallel to one cubic $\langle 001 \rangle$ axes. On the other hand, the tetragonal to monoclinic phase transition is characterized by a martensitic phase transition accompanied by large hysteresis in the phase transition temperature, greater than 200°C, and the generation of large shear and volume elastic strains in the monoclinic phase [16, 17]. It has been observed that the martensitic transformation temperature for the t \rightarrow m can be brought down significantly by adding additives of suitable characteristics which facilitates the stabilization of the tetragonal phase. The monoclinic and tetragonal unit cell of ZrO_2 is shown schematically in figure 1.5.

1.5 Importance of ZrO_2 based materials in catalysis

As discussed earlier, ZrO_2 is an amphoteric oxide which displays surface acid-base properties. The acid-base properties of ZrO_2 have been exploited to carry out many organic reactions on its surface including, dehydration, hydrogen transfer reaction and Friedel Craft alkylation reactions. In addition to its application in industrial applications ZrO_2 has many technological applications as catalyst and promoter in environmental catalytic processes and energy devices. The following is a brief account for application of zirconia as catalyst.

1.6 Surface and structural modification of zirconia

Although ZrO_2 has been used as an acid-base catalyst for numerous organic reactions in heterogeneous catalysis, its application has however been limited by the presence of mild acidic and basic sites on its surface. In this regard recent years, there are many investigations on increasing the surface acid strength of zirconia by surface as well as structural modification. The most prominent among them is anchoring catalytically active metal oxides and anions such as WO_3 , SO_4^{2-} and MoO_3 at submonolayer level to generate newer acidic sites. The results achieved in recent years are quite remarkable considering the fact that strength of the order of 100% H_2SO_4 can be achieved by these modifications which is rarely found in any heterogeneous catalyst. The grafting of sulfated species on ZrO_2 strong acidic sites on their surfaces often termed as “super acidic” which are capable of catalyzing carbonium ion reactions under mild

conditions. The relatively simple method of preparation of these catalysts makes them one of the attractive classes of heterogeneous catalysts. Sulfated metal oxides can be prepared by treatment of the host oxides with sulfuric acids or ammonium sulfate solutions [12].

Tungsten oxide species dispersed on zirconia supports ($\text{WO}_x\text{-ZrO}_2$) comprise another interesting class of solid acids [13]. The strong acid sites originates on these materials when zirconia oxyhydroxide ($\text{ZrO}_x(\text{OH})_{4-2x}$) is impregnated with solutions containing tungstate anions and then oxidized at high temperatures. The addition of a small amount of platinum (<1 wt % Pt) to preoxidized $\text{WO}_x\text{-ZrO}_2$ samples leads to the formation of active, stable, and selective catalysts for *n*-alkane isomerization reactions. The Pt/ $\text{WO}_x\text{-ZrO}_2$ have shown to catalyze efficient hydrogen transfer steps prevent extensive cracking of adsorbed carbocations by limiting their surface lifetimes [14].

1.7 Objective of the present study

The main objectives of the present study is

1. Synthesis of $\text{ZrO}_2\text{-Fe}_2\text{O}_3$ nanocomposite oxides by combustion synthesis using fuels with different valancies such as oxyldihydrazide and malonate dihydrazide.
2. To vary the fuel to oxidized stoichiometry to study the effect of the fuel content and nature on the physicochemical properties of the oxide
3. Characterization of the synthesized materials by using various analytical techniques such as XRD, IR, SEM, Particle size analyzer, UV-Vis to obtain complete information on the physicochemical characteristics of these materials
4. Thermodynamic calculation on the combustion synthesis process to understand the phasetransformation behavior of zirconia.

CHAPTER 2

MATERIALS AND METHODS

2.1 PREPARATION OF CATALYSTS

2.1.1 Preparation of Fe_2O_3 - ZrO_2 catalysts

The ZrO_2 , Fe_2O_3 , and Fe_2O_3 - ZrO_2 composite oxides with 2, 5, 10 and 20 mol% of Fe_2O_3 were prepared by combustion method. Zirconium oxy nitrate ($ZrO(NO_3)_2 \cdot xH_2O$), Ferric nitrate $Fe(NO_3)_3 \cdot 9H_2O$ were used as oxidizer and the oxalyl dihydrazide (ODH) and Malonic acid dihydrazide (MDH) were used as fuel for the combustion synthesis. The reaction stoichiometry (F/O ratio) was calculated using the method described by Jain et al [15]. In a typical synthesis procedure for the preparation of Fe_2O_3 (20 mol%)- ZrO_2 at a reaction stoichiometry of F/O =1 using ODH as fuel, 1.42 g of zirconium oxynitrate, 1.21 g of ferric nitrate and 0.99 g of ODH fuel was dissolved in minimum amount of water to obtain a redox mixture. The redox mixture was kept in a muffle furnace preheated at 400°C. The redox mixture was found to get instantaneously ignited releasing a lot of gaseous products. The combustion residue is subsequently cooled, grinded and calcined at air for 2h to obtain Fe_2O_3 (20 mol%)- ZrO_2 catalysts. The Fe_2O_3 - ZrO_2 composite oxides are referred to as xFeZr-ODH and xFeZr-MDH in the text where x represent the mol% of Fe_2O_3 content in the sample. In order to study the effect of reaction stoichiometry on the physicochemical characteristics of the synthesized materials the F/O ratio was varied from 0.5-1.5 for both ODH and MDH fuel.

2.2 CHARACTERIZATION OF CATALYST MATERIALS

X-ray diffraction: The X-ray diffraction patterns of the xFeZr and 20FeZrS samples were recorded on a Siemens D-500 diffractometer using Ni-filtered CuK_{α} radiation. The XRD measurements were carried out in the 2θ range of 20-70° with a scan speed of 2 degrees per minute using Bragg-Brantano configuration.

Scanning Electron Microscopy: Scanning electron micrograph were taken using JEOL JSM-5300 microscope (acceleration voltage 15 kV). The sample powders were deposited on a carbon tape before mounting on a sample holder for SEM analysis.

UV-Vis Spectroscopy : UV-Vis Spectra of pure ZrO_2 , xFeZr and 20FeZrS materials were recorded using barium sulphate as reference compound on a Shimadzu spectrophotometer (UV-2450) in the range of 200-900nm.

Result and Discussion

3.1 XRD study

Figure 3.1 shows the XRD patterns of the pure zirconia prepared by using oxylyl dihydrazide and malonic acid dihydrazide as fuel. The pure zirconia prepared using either of the fuel shows XRD patterns with 2θ values at 30.2, 35, 50.3 and 59.8 degrees. These peaks correspond to the presence of the tetragonal phase of zirconia. As discussed earlier zirconia exist in three polymorphic forms namely monoclinic, cubic and tetragonal. Out of these three polymorphic forms the tetragonal phase is a metastable form and has many technological applications [10, 11]. There were many studies available in literature regarding the selective stabililzation of the tetragonal phase of zirconia. The conventional method of preparation of zirconia such as precipitation, decpmsition of the precursor salt generally yield a mixture of monoclinic and tetragonal phase. In the present study, the selective formation of the tetragonal phase is a significant observation.

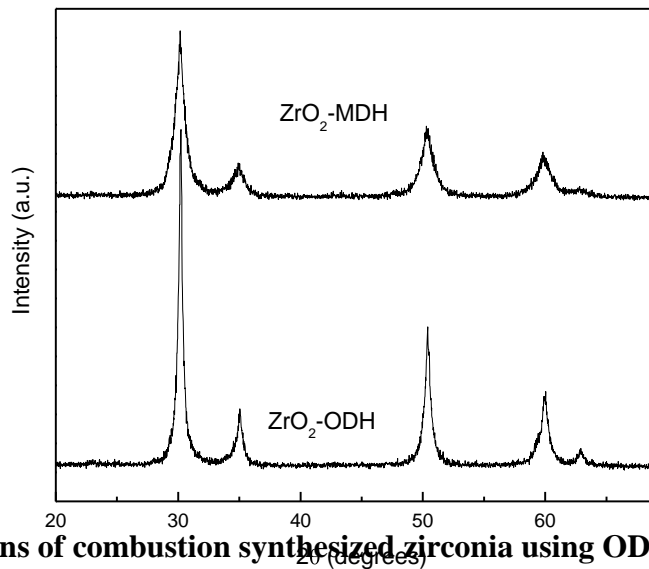


Figure 3.1 XRD patterns of combustion synthesized zirconia using ODH and MDH as fuel.

The combustion method is thus quite effective for the preparation of the metastable phases. Comparison of the XRD profile of the ZrO_2 -ODH and the ZrO_2 -MDH it was observed that the ZrO_2 -ODH are more crystalline with well defined peaks as compared to the ZrO_2 -MDH material. The XRD patterns of the 20FeZr materials prepared by using Oxylyl dihydrazide as fuel are presented in figure 3.2. All the 20FeZr materials prepared by using oxalylyl dihydrazide as fuel found to display peaks corresponding to the presence of tetragonal phase. It was observed that as

the fuel to oxidizer ratio is increased from 0.5 to 1.5 the intensity of the peak at 2θ values at 30.2 is found to increase indicating the formation of well crystalline materials at higher fuel content.

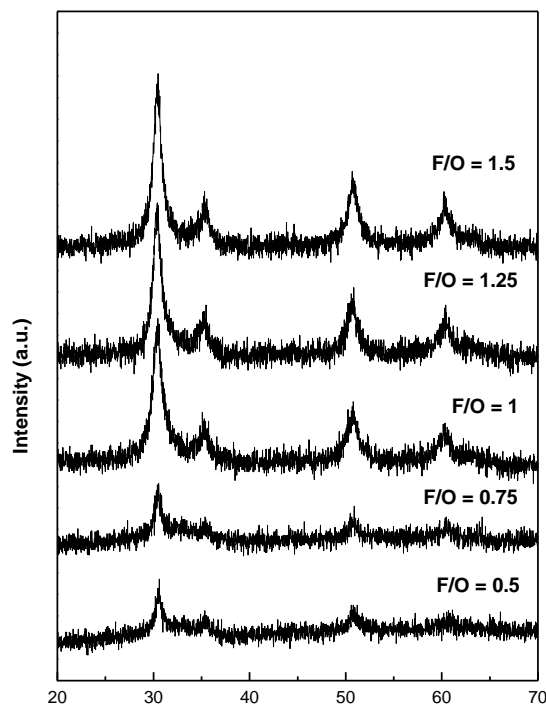


Figure 3.2 XRD patterns of the 20FeZr-ODH materials prepared using different fuel to oxidizer ratio and the 20FeZrS materials.

This is probably due to increase in exothermicity of the reaction with increase in fuel amount in the combustion mixture. No crystalline phase corresponding to the presence of iron oxide was observed in the 20FeZr sample indicating well dispersion of the iron oxide component in the zirconia matrix. The 20FeZrS material on the other hand shows a completely different XRD profile compared to the 20FeZr material. This study clearly shows the effect of different foreign ionic species on the phase transformation behavior of zirconia. The dispersion of iron in zirconia matrix result in the stabilization of tetragonal phase of zirconia. There are many studies available in literature regarding the phase transformation behavior of zirconia [16, 17] . It has been reported that there is a critical crystallite size below which the tetragonal phase of zirconia is stable [16]. The presence of tetragonal zirconia in the present study indicates that the crystallite size of pure ZrO_2 synthesized by combustion method is less than the critical size. The tetragonal phase of zirconia is also stabilized in presence of aliovalent impurity ions in zirconia lattice [13, 16-17]. These ions help restricting the motion of the defects in the lattice thereby stabilizing the

tetragonal phase. In the present study, it is likely that the Fe_2O_3 are anchored to the defect centers. This result in the restriction in the motion of defect centers which facilitates the tetragonal to monoclinic phase transformation. Similar result was observed using MDH as fuel.

3.2 UV-Vis study of the xFeZr composite oxides

The UV-Vis spectra of the pure ZrO_2 along with the xFeZr materials with different Fe_2O_3 content prepared using oxalyl dihydrazide as fuel are presented in Figure 3.4. The pure ZrO_2 prepared by this method shows a sharp and intense band at 212 nm with an absorption edge around 300 nm. ZrO_2 is a direct band gap insulator which shows interband transition in the UV region of the spectrum. The monoclinic form ZrO_2 has two direct interband transitions at 5.93 eV and 5.17 eV, where as the tetragonal form has a band gap of 5.1 eV [18]. In the present case the peak a 212 nm can be assigned to the $\text{O}^{2-} \rightarrow \text{Zr}^{4+}$ charge transfer transition from the tetragonal phase of zirconia. The presence of Fe_2O_3 in the zirconia matrix significantly modifies the UV absorption feature of the zirconium dioxide. The XFeZr materials with low Fe_2O_3 content (2 and 5 mol%) shows a prominent band at 280 nm along with a broad band at 480 nm. The band at 280 nm can be assigned to isolated octahedral Fe^{3+} species anchored to the zirconia surface where as the 480 nm peak can be assigned to the presence of bulk type Fe_2O_3 particles. Iron in Fe^{3+} state is expected to show two ligand to metal charge transfer transitions corresponding to the $t_1 \rightarrow t_2$ and $t_1 \rightarrow e$ transitions [19-22]. However, depending upon the coordination environment of the Fe^{3+} species these transitions differ widely in energies and appear in different region of the spectrum. Ferric ion in a isolated state gives peaks below 300 nm. For example, Fe^{3+} in isomorphously substituted in the silicate frame work shows two peaks at 215 and 241 nm [20]. Similarly, Fe^{3+} in isolated octahedral state shows LMCT transitions around 280 nm in Fe^{3+} doped alumina sample [22]. Thus the CT bands are red shifted as the number of oxygen ions coordinated to the Fe^{3+} increases. It has also been reported in literature that the Fe^{3+} present in small nonstoichiometric nanooxide clusters of the type Fe_xO_y shows charge transfer transition in the range of 300-400 nm where as bulk type Fe_2O_3 particle shows UV absorption above 450 nm. In the present study, the peak at 280 nm can be assigned to the isolated octahedral species anchored to the surface of the zirconia particles. As the Fe_2O_3 content increases, this peak found to be red shifted and reappear in the range of 300-400 nm. With increase in Fe_2O_3 content it is likely that the adjacent sites on the ZrO_2 surface are occupied resulting in lateral linkage between isolated Fe^{3+} species to form small nanoclusters.

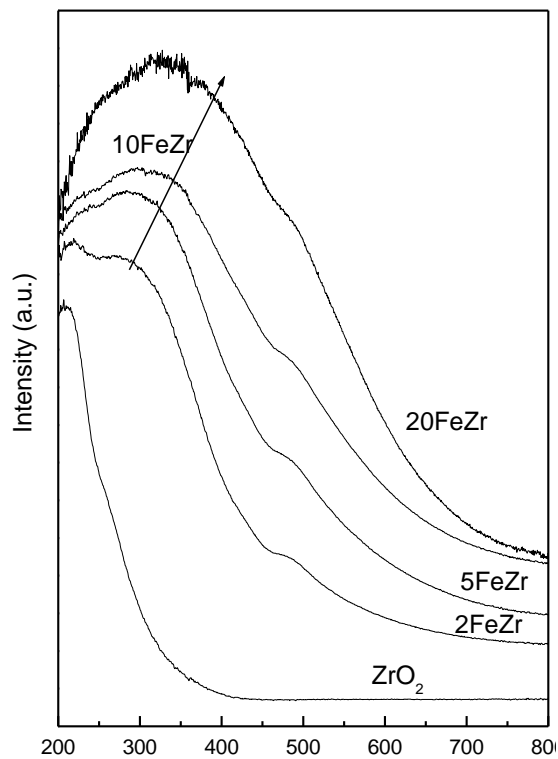
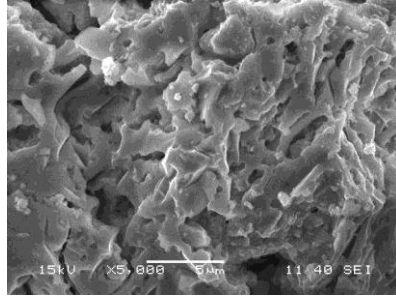


Figure 3.4 UV-Vis spectra of the xFeZr composite oxides prepared using oxalyl dihydrazide as fuel

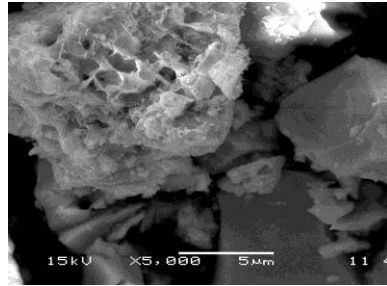
Simultaneously, also it was observed that with increase in iron oxide content the peak at 480 nm gains intensity indicating formation of more bulk type particles. It can be concluded that the combustion synthesized xFeZr materials at low iron oxide loading predominantly contain well dispersed isolated Fe^{3+} species along with some bulk type particles. At higher iron oxide content, the small Fe_xO_y type nanoclusters along with bulk type particles are present on zirconia surface.

3.3 SEM study

The scanning electron micrographs of the 20FeZr materials prepared using combustion synthesis are presented in figure 3.5. The combustion synthesized samples were found to be of low density and spongy in nature. There are numerous micropores present on the surface of the particles. These interparticle pores are due to the escaping gases formed during the combustion process.



(a)



(b)

Figure 3.5 Scanning electron micrograph of 20FeZr-ODH (a) F/O= 0.75 and (b) F/O= 0.5

3.5 Thermodynamic calculation

In order to understand the phase transformation behavior of zirconia in the composite oxide and the thermodynamics of the combustion process calculations were carried out find the standard heat of formation of the composition oxides and the adiabatic reaction temperature. Since combustion reaction takes place in a very short time span, the dissipation of heat to the surrounding is negligible. Under such condition the combustion reaction can be treated as thermally isolated [23, 24] and the adiabatic reaction temperature (the temperature to which the reactants are raised) (T_d) can be calculated from the expression

$$\Delta H_r^0 = \int_{298}^{T_{ad}} C_p(\text{product}) dT \quad \text{----- (1)}$$

Where ΔH_r^0 is the standard heat of reaction and the C_p is the constant pressure heat capacity. The ΔH_r^0 can be calculated from the standard heat of formation of the reactants and products by the expression

$$\Delta H_r^0 = \left(\sum n \Delta H_f^0 \right)_{\text{products}} - \left(\sum n \Delta H_f^0 \right)_{\text{reactants}} \quad \text{-----(2)}$$

The table 3.1 shows the standard heat of formation of the reactants and the products [25, 26]. The temperature dependant Cp values are also given in the table 3.1.

Table 3.1. Standard heat of formation and Cp values of reactants and products.

Compound	ΔH_f^o (kJmol ⁻¹)	Cp value(JK ⁻¹ mol ⁻¹)
ZrO(NO ₃) ₂ .H ₂ O	-1820	----
Fe(NO ₃) ₃ .9H ₂ O	-3285	----
C ₂ H ₆ N ₄ O ₂	-295.2	----
ZrO ₂	-1101.3	69.668+7.53 x 10 ⁻³ T-14.06 x 10 ⁻⁵ T ²
Fe ₂ O ₃	-824.2	31.71+1.76 x 10 ⁻³ T
N ₂	0	27.926 + 4.1868 x 10 ⁻³ T
CO ₂	-393.77	44.17 +9.043x 10 ⁻³ T-8.54 x 10 ⁻⁵ T ²
H ₂ O	-242	30.75+9.16 x 10 ⁻³ T+0.15 x 10 ⁻⁵ T ²

Using the thermodynamic values from Table 3.1, the standard heat of reaction and the adiabatic temperature of the other nanocomposite oxides are calculated and presented in Table 3.2 It can be observed from the table 3.2 that as the iron content increases, the exothermicity of the reaction increases. The adiabatic temperature of the reaction increases with increase in iron content. The adiabatic temperatures of the composite falls in a temperature range where the tetragonal phase is the stable phase. Moreover, the number of moles of the gases increases with increase in iron content. These evolving gases are responsible for the spongy and porous nature of the particles.

Table 3.2 The standard heat of reaction and the Adiabatic reaction temperature of the xFeZr composite oxides

Compounds	ΔH_r^0 (KJmol ⁻¹)	Tad (K)	No of moles of gases
ZrO ₂	-741.46	1941	9.0
2FeZr	-772.1	1992	9.66
5FeZr	-817.78	2074	10.65
10FeZr	-894.03	2256	12.3
20FeZr	-1046.3	2315	15.6

CHAPTER 4

CONCLUSION

The combustion synthesis is used as an effective method for the synthesis of Fe₂O₃-ZrO₂ nanoparticles. The effect of F/O ratio and the nature of the fuel on the physicochemical characteristics of the composite oxide are studied in detail. XRD study indicate the selective stabilization of the tetragonal phase of zirconia. With increase in F/O ratio, the material crystallinity was found to increase for the composite oxide. UV-Vis study indicate the presence of a variety of iron oxide species in the form of isolated, clusters and bulk type particles in the composite oxide. The type OF Fe₂O₃ species present in zirconia depends on the amount of iron oxide loading. SEM study indicate the material to be porous and of low density. Numerous macropores are found to be present on the surface of the particles formed due to the escaping gases. Thermodynamic calculations preformed indicate increase exothermicity of the reaction with iron content. The adiabatic reaction temperature calculated for the composite oxides falls in the range where the tetragonal phase of zirconia is the stable phase.

REFERENCES

1. R.L. Augustine, Heterogenous catalysis for the synthetic chemist. Marcel Dekker Inc, New York, 1996.
2. G.K. Boreskov, *Kinet. Catal.* 14 (1973) 7.
3. T. Seiyama, *Catal. Rev. Sci. Engg.* 34 (1992) 281.
4. K.C. Patil, S.T. Aruna and T. Mimani, *Curr. Opin. Solid State Mater. Sci.* 6 (2002) 507.
5. J. Yang, J. Lian, Q. Dong, Q. Guan, J. Chen, Z. Guo, *Mater. Lett.* 57 (2003) 2792.
6. X. Song and A. Sayari, *Catal. Rev. Sci. Engg.* 38 (1996) 329
7. G. Ranga Rao, *Bull. Mater. Sci.* 22 (1999) 89.
8. W. Stichert, F. Schuth, *Chem. Mater.* 10 (1998) 2020.
9. M. H. Bocanegra-Bernal, S. D'iaz de la Torre, *J. Mater. Sci.* 37 (2002) 4947.
10. M. Shelef, R.W. McCabe, *Catal. Today* 62 (2000) 35.
11. J. Kašpar, P. Fornasiero, N. Hickey, *Catal. Today* 77 (2003) 419.
12. K.Arata, M.Hino, *Appl. Catal.* 59 (1990) 197
13. B.G. Mishra et al, *Colloid and Surfaces A* 317 (2008) 234
14. E.A. El-Sharkawy, A.S. Khder, *Microporous Mesoporous Mater.* 102 (2007) 128.

15. S.R. Jain, K.C. Adiga, V.R. Paivernekar, *Combustion Flame* 40 (1981) 71.
16. E.A. El-Sharkawy, A.S. Khder, *Microporous Mesoporous Mater.* 102 (2007) 128.
17. K. V.R. Chary, K. R. Reddy, G. Kishan, J.W. Niemantsverdriet, G. Mestl, *J. Catal.* 226 (2004) 283.
18. M. Scheithauer, R. K. Grasselli, H. Knzinger, *Langmuir* 14 (1998) 3019.
19. A. Gervasini, C. Messi, P. Carniti, A. Ponti, N. Ravasioe, F. Zaccheria, *J Catal.* 262 (2009) 224.
20. M. Santhosh Kumar, M. Schwidder, W. Grünert, A. Brückner, *J. Catal.* 227 (2004) 384.
21. S. Bordiga, R. Buzzoni, F. Geobaldo, C. Lamberti, E. Giamello, A. Zecchina, G. Leofanti, G. Petrini, G. Tozzola, G. Vlaic, *J. Catal.* 158 (1996) 486.
22. X. Gao, I.E. Wachs, *J. Phys. Chem. B* 104 (2000) 1261.
23. J. Kishan, Venu Mangam, B.S.B. Reddy, Siddhartha Das, Karabi Das, *J. Alloys Compounds* 490 (2010) 631.
24. J.B. Holt, Z.A. Munir, *J. Mater. Sci.* 21(1986) 251.
25. Lange, N.A. and G.M. Forker (Eds.), *Handbook of Chemistry* 10th edition New York: McGraw-Hill, 1967
26. West, R.C. and M.J. Astle (Eds) 1980 *CRC Handbook of Chemistry and Physics*, 61st edition (Boca Raton Florida: CRC Press Inc.) p. D-66.